^{13}C Nuclear Magnetic Resonance Relaxation of Amylose and Dynamic Behavior of the Hydroxymethyl Group

Photis Dais

Department of Chemistry, University of Crete, P.O. Box 1470, 71110 Iraklion, Crete, Greece

R. H. Marchessault*

Department of Chemistry, McGill University, 3420 University Street, Montreal, Quebec, Canada H3A 2A7

Received November 21, 1990; Revised Manuscript Received March 8, 1991

ABSTRACT: The backbone rearrangement and the motion of the exocyclic hydroxymethyl group of amylose in dimethyl sulfoxide using ^{13}C NMR relaxation has been evaluated. The Dejean–Laupretre–Monnerie model appears to be a reasonable basis for the interpretation of the experimental relaxation data corresponding to C(1) to C(5) in the glucopyranose residue. However, the jump model between two preferred conformations provides a more realistic description of the hydroxymethyl group internal motion. The relation between the lifetimes of the states was $\tau_A = 3\tau_B$, indicating that the conformational distribution is gauche–gauche (60%) vs gauche–trans (40%).

The present paper is concerned with the dynamics of the primary hydroxyl or esterified primary hydroxyl group in polysaccharides. ^{13}C NMR relaxation measurements have revealed[1-4] that the C(6) carbon of polysaccharides in solution undergoes relatively faster motion about the C(5)–C(6) exocyclic bond. This conclusion is based on the fact that the T_1 value of the C(6) carbon, bonded to two protons, is longer than the T_1 values observed for the ring carbons. However, this internal motion is expected to be of restricted amplitude due to possible intramolecular and/or intermolecular hydrogen bonding, unfavorable nonbonded, and electronic interactions. Crystallographic studies[5,6] on carbohydrates have shown that the observed conformations for the hydroxymethyl group about the exocyclic bond fall into two general classes, gauche–gauche (60%) and gauche–trans (40%) for the gluco configuration, whereas for the galacto configuration the gauche–trans is preferred (58%) relative to trans–gauche (34%) and gauche–gauche (8%).

Modeling the dynamics of the hydroxymethyl group in linear polysaccharides, three general types of motions are considered: (1) the overall rotatory diffusion, (2) segmental or backbone rearrangement, and (3) internal motion relative to the backbone monomer units. Each of these motions is considered as an independent source of motional modulation of the dipole–dipole interaction, so that the composite correlation function is a product of the correlation functions associated with each motion. For sufficiently high molecular weight polymers, the overall rotatory diffusion is much slower than the chain local motions; thus, it is a negligible contributor to the relaxation of the backbone carbons. In this case, this motion can be safely ignored. For example, the overall motion of an amylose sample in dimethyl sulfoxide ($M_w = 3.3 \times 10^5$) is described by a long correlation time, 7.0×10^{-6} s, as estimated from hydrodynamic measurements.[1]

The second independent motion requires a suitable, dynamic model that reflects the geometric constraints, which characterize the chain flexibility in polysaccharides. No such model exists in the literature based directly on polysaccharide structural details and describing possible modes of reorientation in a carbohydrate chain. The applicability of the Jones and Stockmayer (JS)[7] model to the relaxation of polysaccharides[1,2] appears to be limited, as shown[1] by NMR multifield relaxation experiments. In a recent report,[8] one of us examined the nature of the internal and overall modes of reorientation in amylose dissolved in dimethyl sulfoxide by using a variety of dynamic models on the basis of multifield ^{13}C parameters T_1, T_2, and NOE. Although this treatment was successful in reproducing the relaxation data and particularly the difference between the relaxation parameters of the anomeric carbon from those of the remaining ring carbons and in accounting for the helix-like character of the amylose chain in DMSO, it cannot be generalized to other linear or branched polysaccharides with less pronounced helical segments in solution. Moreover, the complexity of the models used does not allow an easy description of the additional C(6) internal motion.

Recently, Dejean–Lauprêtre–Monnerie (DLM)[9] introduced an effective modification of the conformational jump model as described by Hall–Weber–Helfand (HWH)[10] by taking into consideration local anisotropic motion described by a fast libration of the C–H vectors in addition to segmental motion. The composite orientation autocorrelation function of the DLM model and its Fourier transform, the spectral density, are given in ref 9. In this model, the time scale of chain segmental motions is set by two parameters, τ_0 and τ_1, the correlation times in the HWH model[10] describing single conformational transitions and cooperative conformational transitions, respectively. The librational motion of the C–H vectors has been described[9] in terms of a fast, anisotropic motion occurring with correlation time, τ_2, inside a cone of half-angle Θ, the axis of which coincides with the rest position of the C–H vector.

Table I summarizes the calculated and experimental relaxation data of amylose, the latter taken from refs 1 and 8, and the simulation parameters of the DLM model. Agreement between experimental and calculated values is very good. It should be noted that the τ_1/τ_2 ratio cannot be accurately determined and that good agreement between theory and experiment is obtained insofar as $200 \leq \tau_1/\tau_2 \leq 800$. The simulated values for the angle Θ are 21° for the C(1) carbon and 26° on average for the remaining ring carbons. The different values of Θ explain the fact that the T_1 value for the C(1) carbon is different than those of the other ring carbons, and they support the

0024-9297/91/2224-4611$02.50/0

Table I
Experimental[a] and Calculated[b] Relaxation Parameters for the Ring Carbons of Amylose in Dimethyl Sulfoxide Using the DLM Model[c]

	C(1)	C(2)	C(3)	C(4)	C(5)
			At 20.1 MHz		
T_1[d]	79 (68)	86 (75)	90 (78)	88 (76)	88 (77)
T_2[d]	58 (57)	65 (63)	65 (65)	64 (64)	61 (64)
NOE	2.24 (2.18)	2.20 (2.18)	2.10 (2.18)	2.08 (2.18)	2.12 (2.18)
			At 50.3 MHz		
T_1	127 (128)	150 (141)	154 (146)	144 (143)	151 (145)
T_2	75 (80)	84 (89)	87 (92)	87 (90)	89 (91)
NOE	1.90 (1.93)	1.86 (1.93)	2.02 (1.93)	1.83 (1.93)	1.89 (1.93)
			At 75.4 MHz		
T_1	182 (181)	197 (200)	203 (207)	194 (203)	204 (205)
T_2	105 (103)	119 (116)	119 (118)	115 (115)	117 (116)
NOE	1.58 (1.63)	1.63 (1.63)	1.68 (1.63)	1.59 (1.63)	1.65 (1.63)
			At 100.5 MHz		
T_1	224 (238)	255 (263)	253 (262)	251 (267)	249 (259)
T_2	105 (103)	119 (116)	119 (118)	115 (115)	117 (116)
NOE	1.58 (1.63)	1.63 (1.63)	1.68 (1.63)	1.59 (1.63)	1.65 (1.63)
θ,[c] deg	20.7	26.5	26.8	26.0	26.4

[a] Taken from refs 1 and 8. Experiments were conducted with Bruker WP-80, Varian XL-200 and XL-300, and Bruker WH-400 spectrometers. Probe temperature was 80 ● 0.5 °C. The standard two-pulse recovery technique and the Carr–Purcell–Meiboom–Gill method were used for the measurements of T_1 and T_2, respectively, whereas the "gated decoupling" was employed for the NOE experiments. Samples of wheat starch amylose, 6% (w/v), in Me_2SO-d_6 were degassed by bubbling with nitrogen gas for 2 min before use. The molecular weight of amylose was 3.3×10^5. [b] Values in parentheses. [c] Fitting parameters: $\tau_1 = 9.05 \times 10^{-10}$ s, $\tau_0/\tau_1 = 10$, $\tau_1/\tau_2 = 200$, and values of angle θ as in Table I. [d] In ms.

conclusion that these two types of carbon sites do not experience the same local dynamics. The smaller Θ value for the anomeric carbon indicates a greater steric hindrance to the librational motion of the corresponding equatorial C–H vector relative to that of the axial vectors in the remaining ring sites. Shortening of the C(1)–O(1) and C(1)–O(5) bonds relative to the remaining C–O bonds observed in the crystal structure of amylose[11] and other α-glucopyranosides[5] appears to be a major cause for restricting the amplitude of the local libration at the anomeric carbon.

Modeling the Internal Motion of the Hydroxymethyl Group

Free internal rotation about the C(5)–C(6) exocyclic bond superimposed on the segmental motion as described by a composite autocorrelation function[12] based on the HWH model and the Woessner equations[13] for stochastic diffusion and jump processes cannot reproduce the experimental relaxation data for the C(6) carbon in Table II. Based on the crystallographic data,[5,6] a two-state model may be suitable for describing the relaxation data as a function of an angle, which defines the amplitude of motion. For this reason, we adopt the internal two-state jump model of London,[14] which has been discussed by Jones[15] as well. This model describes internal jumps between two stable states, A and B, with lifetimes τ_A and τ_B. This motion, assumed to be independent, is superimposed on segmental motions, which may be described in terms of conformational jumps by the HWH model. Combining the autocorrelation functions of these two models, we can obtain a new autocorrelation function as

$$G(t) = C_1 \exp(-t/\tau_0) \exp(-t/\tau_1) I_0(t/\tau_1) + C_2 \exp(-t/\tau_0) \exp(-t/\tau_c) \exp(-t/\tau_1) I_0(t/\tau_1) \quad (1)$$

where τ_0 and τ_1 have the same meaning as before and τ_c is the correlation time associated with the two-state jump motion and is given as a function of the lifetimes of the two states.

Table II
Experimental[a] and Calculated[b] Relaxation Parameters for the C(6) Carbon of Amylose in Dimethyl Sulfoxide Using Two Motional Models

	20.1 MHz	50.3 MHz	75.4 MHz	100.5 MHz
	A:[d] HWH Model + Two-State Jump			
T_1[c]	62 (50)	90 (92)	130 (129)	152 (166)
T_2[c]	38 (41)	54 (58)	68 (66)	82 (73)
NOE	2.25 (2.19)	2.02 (1.97)	1.81 (1.83)	1.64 (1.73)
	A:[e] HWH Model + Two-State Jump			
T_1	62 (50)	90 (91)	130 (127)	152 (164)
T_2	38 (42)	54 (59)	68 (63)	82 (74)
NOE	2.25 (2.21)	2.02 (1.99)	1.81 (1.85)	1.64 (1.72)
	B:[f] HWH Model + Restricted Internal Diffusion			
T_1	62 (50)	90 (91)	130 (127)	152 (164)
T_2	38 (42)	54 (58)	68 (68)	82 (74)
NOE	2.25 (2.21)	2.02 (1.99)	1.81 (1.85)	1.64 (1.73)

[a] Taken from refs 1 and 8. Experimental details as in Table I. [b] Values in parentheses. [c] In ms. [d] Input parameters: $\beta = 110°$, $\tau_1 = 9.05 \times 10^{-10}$ s, $\tau_0 = 10\ \tau_1$. Fitting parameters: $\chi = 60°$, $\tau_A = 4.9 \times 10^{-11}$ s, $\tau_A/\tau_B = 3$. [e] Input parameter: $\beta = 110°$. Fitting parameters: $\chi = 65°$, $\tau_0 = 8.75 \times 10^{-9}$ s, $\tau_1 = 7.79 \times 10^{-10}$ s, $\tau_A = 0.90 \times 10^{-11}$ s, $\tau_A/\tau_B = 3$. [f] Input parameters: $\beta = 110°$ Fitting parameters: $\chi = 47°$, $\tau_0 = 8.73 \times 10^{-9}$ s, $\tau_1 = 7.83 \times 10^{-10}$ s, $\tau_i = 0.18 \times 10^{-11}$ s.

$$C_1 = \frac{1}{(\tau_A + \tau_B)^2}\left[\frac{3}{4}\sin^4\beta(\tau_A^2 + \tau_\beta^2 + 2\tau_A\tau_B\cos 4\chi) + 3\sin^2\beta\cos^2\beta(\tau_A^2 + \tau_B^2 + 2\tau_A\tau_B\cos 2\chi) + \left(\frac{3\cos^2\beta - 1}{2}\right)(\tau_A + \tau_B)^2\right] \quad (2a)$$

$$C_2 = \frac{3\tau_A\tau_B}{(\tau_A + \tau_B)^2}\left[\frac{1}{2}\sin^4\beta(1 - \cos 4\chi) + 2\sin^2\beta\cos^2\beta(1 - \cos 2\chi)\right] \quad (2b)$$

$$\tau_C^{-1} = \tau_A^{-1} + \tau_B^{-1} \quad (2c)$$

Here, the angle β is that formed between the C–H vector and the jump axis (C(5)–C(6) bond) and χ is one-half the jump range (i.e., jumps in between $-\chi$ and $+\chi$).

A second model for the movement of the hydroxymethyl group is "restricted-amplitude internal diffusion", i.e., continuous movement of O(6) between two limiting values of χ, which constitutes another important general class of motion. Restricted diffusion about a single axis has been solved analytically,[16,17] and the resulting autocorrelation function can be combined with the HWH autocorrelation function to give a new autocorrelation function:

$$G(t) = \sum_{a=-2}^{+2}\sum_{n=0}^{\infty}|\mathbf{d}_{a0}(\beta)|^2|\mathbf{E}(a,n)|^2 \exp(-t/\tau_0) \times \exp(-t/\tau_n) \exp(-t/\tau_1) I_0(t/\tau_1) \quad (3)$$

where

$$\tau_n^{-1} = \frac{n^2\pi^2}{24\tau_i\chi^2}$$

Here β is the angle between the relaxation vector (C–H bond) and the internal axis of rotation (C(5)–C(6) bond), 2χ defines the allowed range of motion, τ_i is the correlation

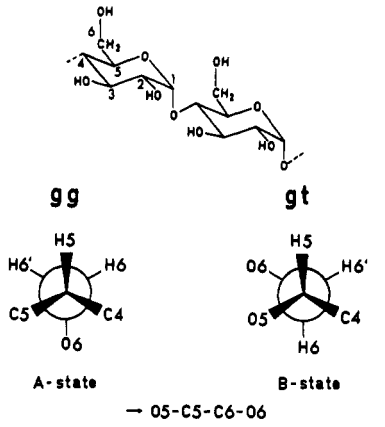

Figure 1. Schematic representation of a disaccharide residue of amylose and Newman-type projections showing the two states A and B corresponding to the gauche–gauche and gauche–trans conformations of the hydroxymethyl group. The jump axis is the C(5)–C(6) exocyclic bond. The range of jumping is ca. 2χ = 120°.

time associated with internal motion, $\mathbf{d}_{i0}(\beta)$ is the reduced Wigner rotation matrix,[18] and the matrix (**E**(i,n) is given in ref 16.

Both models are able to reproduce the experimental data of the C(6) carbon of amylose in Table II, although they differ in the time scale and the range of the restricted motion. For reasons discussed in the Appendix the two-state model is favored. Furthermore, this model appears more realistic for describing the nature of the motion of the hydroxymethyl group in its two preferred conformations (Figure 1), in accord with crystallographic data.[5,6] The longer lifetime, τ_A ($\tau_A = 3\tau_B$), derived by the two-state model (Table II) may be ascribed to the most stable gauche–gauche conformation (60%) as compared to the gauche–trans (40%) state for the gluco configuration.

It should be noted that the DLM model was successful in reproducing the relaxation data of the hydroxymethyl carbon of amylose with fitting parameters $\tau_1 = 8.2 \times 10^{-10}$s, $\tau_0/\tau_1 = 10$, $\tau_1/\tau_2 = 200$, and $\Theta = 33°$.

In summary, the present study attempted to describe the backbone rearrangement and the motion of the exocyclic hydroxymethyl group of amylose in dimethyl sulfoxide solution. The DLM model appears to be a reasonable basis for the present analysis, whereas the two-state model between two preferred conformations may represent a realistic description of the hydroxymethyl group internal motion. However, no activation energies associated with the various local motions can be derived from the present multifield relaxation data. Therefore, variable-temperature measurements of the relaxation parameters for amylose at different magnetic fields should be carried out. Additional experiments on other linear polysaccharides, e.g., cellulose, and on model systems such as cyclomaltoses, whose value in helping interpret the ^{13}C CP/MAS spectra of amylose hydrates is well established,[19] are currently in progress.

Acknowledgment. Financial assistance from the Natural Science and Engineering Research Council of Canada and Xerox is appreciated. P.D. thanks the University of Crete for granting a leave of absence.

Appendix: Numerical Calculations

All numerical calculations and fits to experimental data of amylose were achieved by using the Moldyn program,[20] modified to include the aforementioned motional models. Details for the optimization procedure and other aspects of the program can be found elsewhere.[8,12,21] The fitting of the experimental data in Table I to the DLM function was obtained as follows: initially, the multifield T_1, T_2, and NOE parameters for the C(1) carbon were used as an input, and the best fits for correlation time τ_1 and angle Θ were calculated while the correlation time ratios τ_0/τ_1 and τ_1/τ_2 were varied stepwise by 1 and 20 units, respectively. In subsequent calculations for the remaining ring carbons, the parameters τ_0/τ_1, τ_1/τ_2, and τ_1 obtained from the anomeric carbon were kept constant, while the Θ angle was optimized.

The data in Table II were reproduced either by optimizing all parameters involved in each spectral density function or holding τ_0 and τ_1 at the values determined from the ring carbon data, while adjusting the angle χ and the correlation times for internal motion. Both optimization procedures show similar reproducibility of the experimental data in Table II, although the latter method is preferred so far as it requires fewer adjustable parameters.

The behavior of NT_1, NT_2, and NOEs as a function of the parameters involved in the two previous models describing internal motion has been examined as well through the following equations:

$$\frac{1}{NT_1} = \frac{\hbar^2\gamma_C^2\gamma_H^2}{10r_{CH}^6}[J(\omega_H - \omega_C) + 3J(\omega_C) + 6J(\omega_H + \omega_C)] \quad (1A)$$

$$\frac{1}{NT_2} = \frac{\hbar^2\gamma_C^2\gamma_H^2}{20r_{CH}^6}[4J(0) + J(\omega_H - \omega_C) + 3J(\omega_C) + 3J(\omega_H) + 6J(\omega_H + \omega_C)] \quad (2A)$$

$$\mathrm{NOE} = 1 + \frac{\gamma_H}{\gamma_C}\left[\frac{6J(\omega_H + \omega_C) - J(\omega_H - \omega_C)}{J(\omega_H - \omega_C) + 3J(\omega_C) + 6J(\omega_H + \omega_C)}\right] \quad (3A)$$

Numerical results for NT_1 using the bistable model showed the same behavior as in ref 14 when calculated NT_1 values were plotted as a function of the relative magnitude of the lifetimes $\tau_A = \tau_B$, the correlation times, τ_0 and τ_1, describing segmental motion and the jump range, 2χ. Normal behavior was observed for NT_2 and NOE values in relation to the aforementioned model parameters.

Numerical calculations for the relaxation parameters using the restricted internal diffusion model showed that NT_1, NT_2, and NOE values are monotomic increasing functions of the range of motion, 2χ, for 10^{-7} s $\leq \tau_0 \leq 10^{-6}$ s and 10^{-8} s $\leq \tau_1 \ll 10^{-9}$ s, $\tau_i = 10^{-10}$–10^{-12} s, and β = 109.47°, whereas NT_1 decreased for values $\tau_0 \geq 10^{-6}$ s and $\tau_1 \geq 10^{-7}$ s. This behavior is similar to that observed in ref 16. Nevertheless, a high discrepancy was found between the calculated relaxation parameters corresponding to a full range of motion, i.e., $2\chi = 360°$, and the parameters derived by using the free internal rotation model. Since this important criterion[16] for application of this model is not fulfilled, we discard this motional description from the present analysis despite the fact that it fits the experimental relaxation data.

References and Notes

(1) Dais, P. *Macromolecules* **1985**, *18*, 1351.
(2) Matsuo, K. *Macromolecules*, **1984**, *17*, 449.
(3) Vignon, M.; Michon, F.; Joceleau, J.-P. *Macromolecules* **1983**, *16*, 835.
(4) Perlin, A. S.; Casu, B. In *The Polysaccharides*; Aspinall, G. O., Ed.; Academic Press: New York, 1982; Vol. 1; Chapter 4.

(5) Sundaralingam, M. *Biopolymers* **1968**, *6*, 189.
(6) Marchessault, R. H.; Perez, S. *Biopolymers* 1979, 18, 2369, and references therein.
(7) Jones, A. A.; Stockmayer, W. H. *J. Polym. Sci., Polym. Phys. Ed.* **1977**, *15*, 847.
(8) Dais, P. *Carbohydr. Res.* **1987**, *160*, 73.
(9) Dejean de la Batie, R.; Lauprêtre, F.; Monnerie, L. *Macromolecules* **1988**, *21*, 2045.
(10) Hall, C. K.; Helfand, E. *J. Chem. Phys.* **1982**, *77*, 3275. Weber, T. A.; Helfand, E. *J. Phys. Chem.* **1983**, *87*, 2881.
(11) Winter, W. T.; Sarko, A. *Biopolymers* **1974**, *13*, 1461; **1974**, *13*, 1447.
(12) Dais, P.; Nedea, M. E.; Morin, F. G.; Marchessault, R. H. *Macromolecules* **1989**, *22*, 4208.
(13) Woessner, D. E. *J. Chem. Phys.* **1962**, *36*, 1. Woessner, D. E., Snowden, B. S., Jr.; Meyer, G. H. *J. Phys. Chem.* **1969**, *50*, 719.
(14) London, R. E. *J. Am. Chem. Soc.* **1978**, *100*, 2678.
(15) Jones, A. A. *J. Polym. Sci. Polym. Phys. Ed.* **1977**, *15*, 863.
(16) London, R. E.; Avitabile, J. *J. Am. Chem. Soc.* **1978**, *100*, 7159.
(17) Gronski, W. *Makromol. Chem.* **1979**, *180*, 1119.
(18) Rose, M. E. *Elementary Theory of Angular Momentum*; Wiley: New York, 1957; Chapter 4.
(19) Veregin, R. P.; Fyfe, C. A.; Marchessault, R. H. *Macromolecules* **1987**, *20*, 3007.
(20) Craik, D. J.; Kumar, A.; Levy, G. C. *J. Chem. Int. Comput. Sci* **1983**, *1*, 30.
(21) Dais, P.; Nedea, M. E.; Morin, F. G.; Marchessault, R. H. *Macromolecules* **1990**, *23*, 3387.

Registry No. Amylose, 9005-82-7.